PEDESTRIAN HEAD IMPACT DYNAMICS: COMPARISON OF DUMMY AND PMHS IN SMALL SEDAN AND LARGE SUV IMPACTS

Jason Kerrigan[1]
Carlos Arregui[2]
Jeff Crandall[1]
[1]University of Virginia Center for Applied Biomechanics
United States
[2]European Center for Injury Prevention, Universidad de Navarra
Spain
Paper Number 09-0127

ABSTRACT

This study compares head impact dynamics between post mortem human surrogates (PMHS) and the Polar-II pedestrian crash dummy in vehicle-pedestrian impacts with a small sedan and a large SUV. A total of fifteen (8 sedan, 7 SUV) full-scale vehicle pedestrian impact tests were performed at 40 km/h. For each vehicle, two (SUV) or three (sedan) PMHS tests and five dummy tests were performed, with three of the dummy tests in the same configuration to show repeatability, and the other two tests utilizing slightly different configurations. Head linear and angular kinematics were captured from PMHS and dummy head instrumentation, and dummy neck forces and impact forces were calculated from the upper neck load cell data. Differences in head impact locations, timing, and kinematics between the dummy and PMHS were minimized when the dummy was positioned higher above the ground reference level to match the pelvis height of the PMHS. On average, the dummy recorded higher resultant impact forces (2930 N vs. 1862 N) in windshield impacts to the sedan than in hood impacts to the SUV, which resulted in higher HIC15 values and higher peak and averaged angular accelerations. While differences in dummy injury risk metrics both the dummy and PMHS data show that the difference in injury risk metrics predicted by the dummy can be explained by the variation in impact velocity between the sedan (14.1 ± 1.2 m/s) and the SUV (10.7 ± 2.3 m/s), the differences in injury risk predicted by the PMHS is not as clear due to confounding factors. The data and analyses presented in this study also show that neck forces during head impacts contribute a substantial and additive effect to the head impact accelerations (and thus HIC15 values) measured in the dummy, and that for the SUV, neck forces affect head accelerations more than impact forces. Despite analyzing only lateral impacts with two vehicle geometries at 40 km/h, this study provides the only comparison of PMHS and dummy pedestrian head impact kinematics data available.

INTRODUCTION

Head injuries are either the most or second most commonly reported injuries to pedestrians struck by vehicles (Kong et al. 1996, Edwards and Green, 1999, Peng and Bongard, 1999, Chidester and Isenberg, 2001, Mizuno 2003, Toro et al. 2005, Neal-Sturgess et al. 2007). Furthermore, among serious or life-threatening head and brain injuries far outnumber injuries to all other body regions (Chidester and Isenberg, 2001, Fildes et al. 2004). Previous studies have shown that head and neck injuries sustained by pedestrians account for almost 60% of all Harm to pedestrians (Fildes et al. 2004).

In an effort to mitigate the risk of head (and other) injuries to pedestrians, researchers have developed tools, like pedestrian dummies and computational models, to further understand the dynamics of vehicle-pedestrian impact. While the local stiffness of the individual vehicle structures involved in head-to-vehicle impact is a primary concern in decreasing the risk of head injury, impact simulations with pedestrian dummies and computational models allow for examination of other factors that affect head injury risks. For instance, the magnitude of the accelerations sustained by the head in head-to-vehicle impacts is dictated not only by the vehicle stiffness, but by the impact velocity and impact angle, which dictate the magnitude and duration of the impact forces applied to the head. Additionally, Okamoto and Kikuchi (2006), in a study that involved vehicle-pedestrian impacts with the Polar-II pedestrian dummy, used the dummy's neck instrumentation to explore the magnitudes of forces applied to the head through the neck during impact. Since their goal was to compare pedestrian dummy impacts to those of headform impactors, Okamoto and Kikuchi used neck forces to examine similarities and differences between the dummy and the impactor, without examining how neck forces directly affect impact kinematics and estimates of injury risk.

The current study aims to examine how both the impact and neck forces applied to the head during head-to-vehicle impact influence linear and angular impact kinematics. Furthermore, this study uses both the Polar-II dummy, which has been compared to PMHS in previous tests to verify overall kinematic biofidelity (Akiyama et al. 2001, Kerrigan et al. 2005a, Kerrigan et al. 2005b), and PMHS to further examine not only the biofidelity of the dummy but the limitations of the PMHS model. Lastly, this study examines impacts with two vastly different shaped vehicles, a small sedan and a large SUV, to help elucidate the effects vehicle shape has on head impact dynamics.

METHODS

Vehicle-Pedestrian Impact Experiments

A total of 15 vehicle-pedestrian impact tests with a late-model small sedan (n=8) and a late model large SUV (n=7), using both PMHS (n=5) and the Polar-II dummy (n=10) (Table 1). The methodology and some results from 11 of the 15 experiments have been previously presented (Kerrigan et al. 2005a, Kerrigan et al. 2005b, Kerrigan et al. 2008b). Since the current study presents previously unpublished results from these experiments, as well as results from previously unpublished experiments, the following description will provide a general overview of the test methodology, but focus specifically on the methods associated with the previously unpublished results. For a more complete description of all of the methods used to perform the experiments, the previous studies should be referenced.

Table 1. Test matrix.

	Test ID	Subject	Age/ Gender	Mass (kg)	Stature (cm)	Stance/ Support/ Clothing	Ground Level (cm)
Sedan	D1	Dummy		75	173	Dummy	0
	D2	Dummy		75	174	Dummy	0
	D3	Dummy		75	174	Dummy	0
	DA1	Dummy		75	174	PMHS	0
	DA2	Dummy		75	179	PMHS	+5
	P1	PMHS	61/F	80.7	187	PMHS	0
	P2	PMHS	70/M	54.4	179	PMHS	0
	P3	PMHS	62/M	81.6	186	PMHS	0
SUV	D1	Dummy		75	173	Dummy	0
	D2	Dummy		75	172	Dummy	0
	D3	Dummy		75	171	Dummy	0
	DA1	Dummy		75	174	PMHS	0
	DA2	Dummy		75	179	PMHS	+7
	P1	PMHS	75/F	46.7	177	PMHS	0
	P2	PMHS	53/M	104.2	176	PMHS	0

Sled System Drivable production versions of the vehicles were cut just rearward of their B-pillars, their wheels were removed and their suspensions were locked. The vehicles were welded to a sled sub-frame and ballasted up to the vehicle curb weight for the sedan (1176 kg) and to the sled system limit (1600 kg) for the SUV. Computational simulations verified that only negligible differences in vehicle pedestrian impact dynamics resulted from using an SUV mass less than the vehicle's curb weight. Each vehicle buck was attached to the carriage mounted to the deceleration sled system (Via Systems Model 713, Salinas, CA) at the University of Virginia (UVA) Center for Applied Biomechanics (CAB). Damaged or deformed vehicle components were repaired or replaced between each test.

A small, light pedestrian sled that mimicked the vehicle's ground-reference-level was constructed and attached to the sled system to facilitate surrogate positioning prior to each test. Plywood, which has been shown to possess frictional characteristics similar to that of road surfaces (Kam et al. 2005), was used as the shoe-contact surface on the ground-reference-level of the pedestrian sled. A hydraulic decelerator programmed to decelerate the vehicle and pedestrian sled approximately 250 ms after initial vehicle-pedestrian contact was installed at the end of the sled system to provide a constant 6g deceleration. Above the decelerator, an energy absorbing catching mechanism (Kam et al. 2005) was installed to catch the subject, prohibit ground contact, and prevent additional injuries.

Subject Preparation Three male and two female PMHS (Table 1) were selected for this study based on the absence of pre-existing fractures, lesions, or other bone pathology as confirmed by computed tomography (CT) scan. The PMHS were obtained and treated in accordance with the ethical guidelines established by the Human Usage Review Panel of the National Highway Traffic Safety Administration, and all testing and handling procedures were reviewed and approved by the CAB Biological Protocol Committee and an independent Oversight Committee at UVA. Specimens are labeled (Table 1) by the order of testing (with "P" indicating PMHS).

Each specimen was instrumented with a (6) six-degree-of-freedom (6DOF) cube to facilitate head kinematics measurement during the experiments (Kerrigan et al. 2008a). The 6DOF cube contained three linear accelerometers (model 7264B-2000, Endevco Corp., San Juan Capistrano, CA) and three magnetohydrodynamic (MHD) angular rate sensors (model ARS-06, Applied Technology Associates,

Albuquerque, NM). The six sensors were arranged in a specially designed aluminum cube to permit linear acceleration and angular rate measurements about three orthogonal axes (Figure 1). An aluminum plate (44 x 46 x 5 mm) was attached to the posterior-superior aspect of the skull with deep threaded wood screws (Figure 1). Following preparation, each specimen underwent a computed tomography (CT) scan (0.97 mm/pixel, 1.25 mm slice thickness) to document the orientations of the cube mounting hardware (Figure 1).

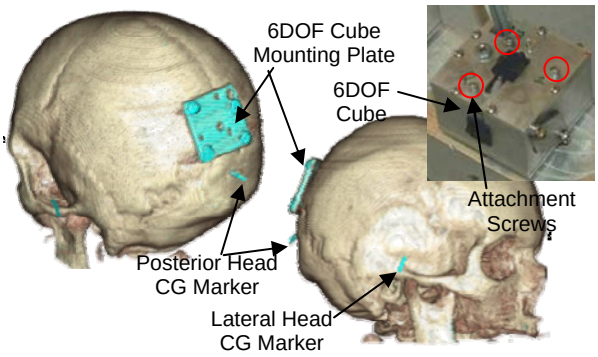

Figure 1. CT scan reconstructions (top) and photograph (bottom) showing 6DOF cube (also inset), cube mounting plate, and markers used to determine head CG. Photograph shows PMHS prone in tray.

The Polar-II dummy was prepared as specified by its developers (e.g. Akiyama et al. 2001). The dummy, which has the head of the Hybrid-III dummy, was instrumented with a nine-accelerometer package (NAP) centered about the head center of gravity using the same geometry as that used in the Hybrid-III. Additionally, the dummy's neck was based on the THOR neck, and thus had a 6-axis upper neck load cell identical to that used in the THOR.

Stance, Support and Clothing Tests were performed in the following order:

1) Repeated dummy tests with each vehicle-"D1", "D2", and "D3" in Table 1,
2) PMHS tests with each vehicle-"P1", "P2", and "P3" in Table 1, and
3) Adjusted dummy tests-"DA1" and "DA2" in Table 1.

Each of the three series of tests were performed with different stance, support, and clothing of the subject (Figure 2). In the first series of tests (repeated dummy tests) the dummy wore its standard jacket, shorts and shoes as specified by its developers. It was supported for positioning by using a single rope that passed through the dummy's shoulder eyebolts (bilaterally) and through the release mechanism. In positioning the dummy in mid-stance gait, the following goals were applied (Kerrigan et al. 2005a):

1) Both right and left thighs oriented at the same angle relative to the ground and no more than 85 degrees from horizontal,
2) Right leg back (struck side) and left leg forward
3) Both feet flat on the ground reference level with the back of the right heel and front of the left shoe tip equidistant from the vehicle centerline
4) Both knees at 0 degrees flexion.

However, due to limited range of motion of the dummy's right hip (it could not be extended more than 5 degrees from neutral), and that the shoulder eyebolts were anterior to the dummy's CG (and thus the dummy's weight was not supported through its CG), achieving goal #3 was impossible without pushing the pelvis back and creating an angle of the thorax relative to the ground (Figure 2).

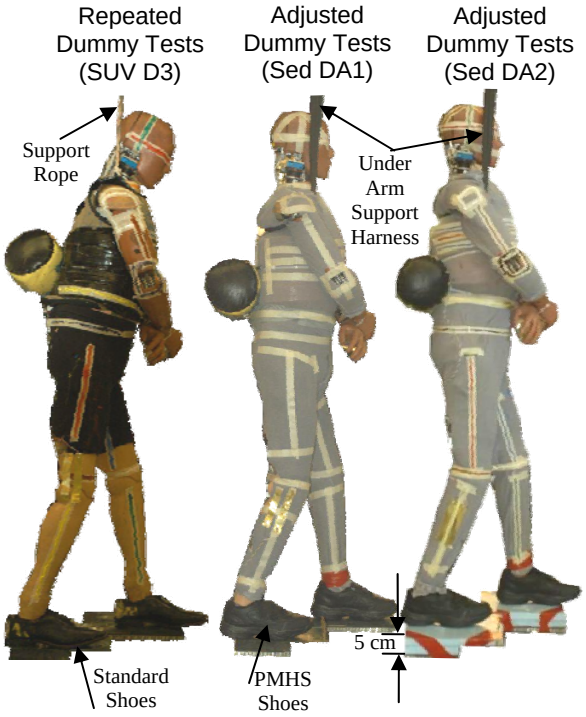

Figure 2. Images from SUV D3 (left), Sed DA1 (middle) and Sed DA2 (right) depicting differences in dummy stance, support and clothing from the three different test series.

The PMHS were outfitted in a TYVEK ® body suit (interior), a cotton/lycra shirt and pants (exterior), a cotton/lycra head cover, and a pair of athletic shoes (Figure 3). The PMHS were supported via a piece of seat belt webbing that passed under the arms anteriorly and across the back posteriorly. Additionally, the PMHS head was positioned with a second piece of

seatbelt webbing that was split and passed under the chin and under the occiput. An attempt was made to position the PMHS like the dummy in the repeated dummy tests, however relatively low stiffness in the hip and knee joints prevented the right hip and right knee from being extended. Gravity drew the right hip and knee into flexion, and the thorax into an orientation perpendicular to the ground.

Figure 3. Images from sedan (left) and SUV (right) PMHS tests depicting PMHS stance, support and clothing.

A number of differences between in pedestrian response between the PMHS and dummy were noted (see Results) and thus a subsequent set of tests were performed with the dummy to determine if the differences were related to the differences in stance, support and position. Since the dummy showed repeatable results in the repeated dummy tests (Kerrigan et al. 2005a, Kerrigan et al. 2005b), only single dummy tests (n=2 for each vehicle) were performed to examine the sensitivity to stance, support and clothing. In the first test on each vehicle (Sed DA1 and SUV DA1), the dummy was outfitted in the same cotton/lycra shirt and pants, and the same athletic shoes used in the PMHS tests (Figure 2). The dummy was not supported using the shoulder eyebolts, but instead was supported with the seatbelt webbing that passed under the arms anteriorly and across the back posteriorly. This support allowed the dummy to be positioned in the same stance as the PMHS: slight flexion in the right hip and thorax perpendicular to the ground reference level. These PMHS-like conditions of the stance, support and clothing are indicated in Table 1 as "PMHS".

In addition to the differences between the PMHS and repeated dummy tests with respect to the stance, support and clothing, all of the PMHS were taller than the dummy (Table 1) as determined by measuring the distance between the top of the head and the ground reference level after positioning each subject. Thus, in an attempt to evaluate how differences in stature affected the response characteristics, in the second of the adjusted dummy tests (Sed DA2 and SUV DA2) the vertical position of the ground reference level was increased using a rigid foam to position the dummy higher up than in the DA1 tests (Figure 2). Since, it has been hypothesized that the height of the pelvis and greater trochanter relative to the vehicle front end components has a larger effect on pedestrian impact kinematics than pedestrian stature (Kerrigan et al. 2005a, Kerrigan et al. 2005b, Kerrigan et al. 2007), the ground reference level height was increased to match the pelvis height of the PMHS. The average height of the PMHS in the sedan tests and SUV tests was approximately 5 cm and 7 cm higher than the height of an analogous point measured on the dummy after positioning in Sed DA1 and SUV DA1, respectively. Thus the ground level for the DA2 tests was adjusted accordingly.

Final Preparation and Test Event Before hoisting PMHS specimens, the 6DOF cube was fixed to the mounting plate, and digitized relative to skull landmarks with a coordinate measurement machine (CMM) (FARO Technologies, Lake Mary, FL). The support harness from each subject was attached to a solenoid release mechanism that supported the weight of the subject until immediately prior to the impact. The subjects were positioned such that the right lateral side facing the vehicle with the support aligned with the vehicle centerline. The upper extremities of the surrogate were bound at the wrist, anterior to the body, with the left wrist closest to the abdomen, to ensure repeatable kinematics and the most severe impact (Kam et al. 2005). Once the final position of the surrogate had been set, the CMM was used to digitize anatomical landmarks used to define the exact position and orientation of the subjects. Additionally, the dummy head and the three attachment screw centers of the PMHS 6DOF cube were digitized to determine the pre-impact global reference frame orientation of the head instrumentation systems.

The test event was initiated by a pneumatic propulsion system that accelerated the vehicle sled to 40 km/h.

The vehicle sled passed an inductive sensor on the track that triggered the release of the surrogate approximately 20 ms before the initial bumper-lower extremity contact. Vehicle-PMHS interaction continued for 250 ms after bumper contact, at which time the vehicle was decelerated (constant ~6 g) and the surrogate was thrown forward into the catching mechanism. All subject-mounted sensor data were sampled at 10 kHz via a wireless data acquisition system (TDAS G5, DTS, Seal Beach, CA). A hardware filter of 3300 Hz was applied during acquisition, and the data were subsequently filtered (CFC 1000) for further processing. The angular rate sensor data were compensated, using a routine specified by the manufacturer (ATA 2008), to extend the effective low frequency corner of the MHD angular rate sensor.

Head Impact Dynamics

Kinematics PMHS head impact kinematics in both the local (body-fixed) and global (inertial) reference frames were calculated at the head CG using established techniques (Rudd et al. 2006, Kerrigan et al. 2008a, Kerrigan et al. 2008b). The location and orientation of the head CG relative to the 6DOF cube was determined by digitizing the cube attachment screws and the posterior and lateral projections of the head CG, which were determined from the Frankfurt plane (based on data from Robbins et al. 1983), prior to positioning the PMHS (Figure 1). Local frame kinematics were determined by first transforming the cube sensor measurements to a reference frame defined by the anatomical axes of the head (adhering to SAE J211), and then by translating cube accelerations first from the surface to the center of the cube, and then to the head CG by applying the rigid body dynamics equation.

The cube's initial global reference frame orientation was determined from the pre-test CMM data. Data from the angular rate sensors were used to update the global frame orientation of the cube at each time step of the impact interaction. By updating the orientation of the cube at each time step, the local sensor data could be expressed in the global reference frame. The components of the global linear velocity vector were determined by integrating the transformed accelerations, and transformed into the vehicle reference frame by using the vehicle velocity time history. Angular acceleration data were determined by differentiating the transformed angular velocity data. To remove the high frequency noise introduced by the numerical differentiation, a 300 Hz (-6 dB cutoff) low-pass second-order Butterworth filter was applied to the angular acceleration data (Rudd et al. 2006).

In the dummy, the components of the local frame angular acceleration vector were calculated from the NAP data (Padgaonkar et al 1975). Angular accelerations were integrated to determine the components of the local frame angular velocity vector. Then the components of the local frame acceleration vector were determined by translating the accelerometer measurements to the head CG using the rigid body kinematics equation. Then, using the same methods as in the PMHS, global reference frame kinematics (linear and angular accelerations, and linear and angular velocities) were calculated.

Impact Forces The time history of the components of the force acting on the dummy head by the vehicle (impact force) can be calculated by applying Newton's second law to the dummy's head (Figure 4). The dummy's head can be modeled as a rigid body with mass m_{head} that accelerates (**a**) as a result of the forces acting on it. In vehicle-pedestrian impacts, a force is applied to the dummy's head through its connection to its neck ($\mathbf{F_N}$), and another force to the head through its contact with the vehicle ($\mathbf{F_I}$). In some cases, more than one force can act on the head by the vehicle (multiple contact locations), however for the purposes of this analysis, the vector sum of these forces is assumed to be only a single force, acting at a single location.

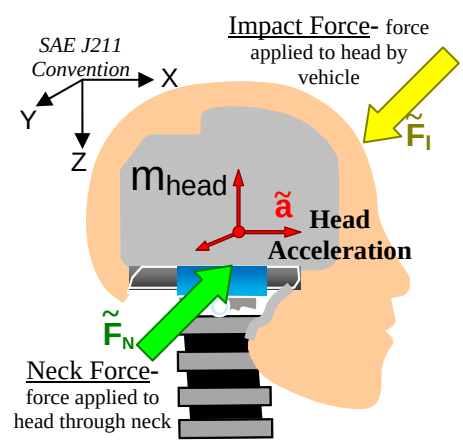

Figure 4. Free body diagram of the dummy's head with component sign convention.

Thus we have the vector relations

$$m_{head}\mathbf{a} = \mathbf{F_I} + \mathbf{F_N} \qquad (1), \text{ and}$$

$$\mathbf{F_I} = m_{head}\mathbf{a} - \mathbf{F_N} \qquad (2).$$

Time histories of the components of the impact force vector were calculated in each dummy test, using Equation 2 with the neck load cell forces and the components of the local frame acceleration vector.

The neck forces and impact forces were calculated as forces applied to the head and with the SAE J211 sign convention (Figure 4).

RESULTS

Linear Kinematics

All sedan impacts resulted in head impact with the vehicle's windscreen and all SUV impacts resulted in head impact with the vehicle's hood (Figure 5). Subjects that were taller, or raised off the ground reference level (both DA2 tests), experienced head contacts farther up the vehicle than shorter subjects. In other words, while the relationship is clearly a function of vehicle geometry, specimen stature was positively (generally) correlated with wrap-around-distance (WAD) to the location of head impact for each vehicle (Table 2 and Figure 6). WAD measurements were made using the standard method of measuring vertically from the ground up to the vehicle bumper, and then along the contour of the vehicle to the head impact location.

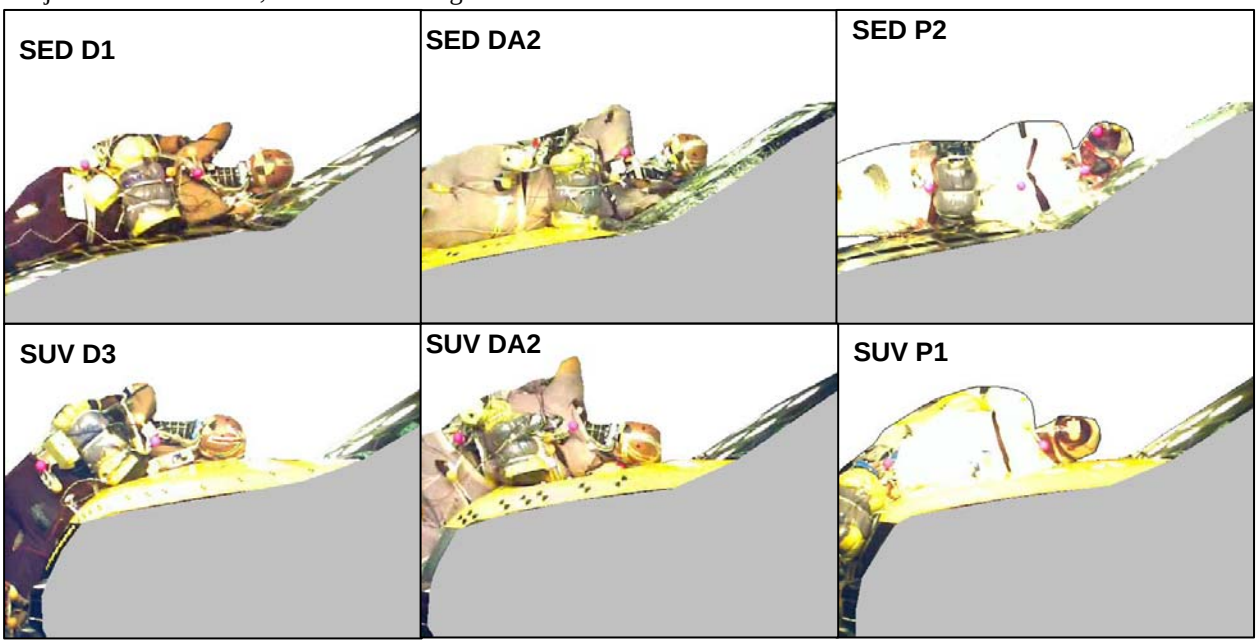

Figure 5. High speed video images depicting the imager frame just prior to impact (HC1) from six of the tests.

Table 2. Head impact parameters for each subject.

Test	WAD (mm)	Impact Velocity (m/s)	HIC15	t1-HIC15 (ms)	t2-HIC15 (ms)	HC1 (ms)	HC2 (ms)
Sed D1	1930	14.69	1437	123.6	138.6	124	125
Sed D2	1940	13.30	1447	122.3	137.3	123	124
Sed D3	1970	13.88	1321	125.4	140.4	127	128
Sed DA1	1970	15.89	1749	122.6	137.6	122	123
Sed DA2	2130	15.31	1091	131.4	146.4	133	134
Sed P1	2410	13.56	824	147.3	162.3	151	152
Sed P2	2200	14.48	3647	135.3	139.4	134	135
Sed P3	2320	11.80	511	138.8	153.8	141	142
SUV D1	1685	9.29	577	92.4	107.4	98	99
SUV D2	1660	10.45	826	85.2	100.2	93	94
SUV D3	1665	9.29	752	84.7	99.7	93	94
SUV DA1	1700	11.39	1704	87	102	93	94
SUV DA2	1850	12.03	1642	94.8	109.8	99	100
SUV P1	1860	12.11	3694	96.8	101.8	95	96
SUV P2	1845	10.64	745	85.9	100.9	91	92

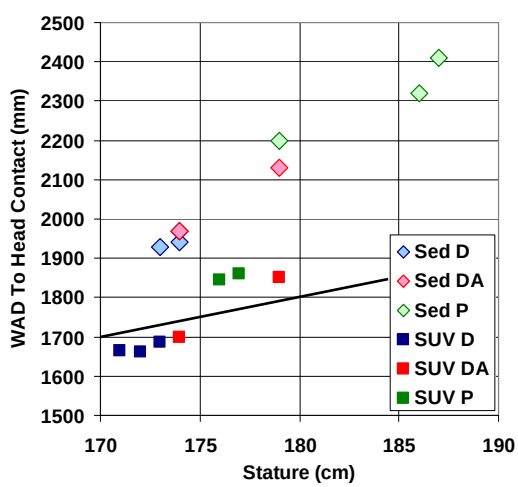

Figure 6. WAD to Head Contact vs. stature for all tests. The black line indicates a WAD equal to stature.

In the case of the sedan, all WAD measurements were greater than stature (Figure 6), which suggests that subjects slide up the vehicle prior to head contact, with the amount of sliding also positively correlated with stature. The repeated dummy tests and the first adjusted dummy test (DA1) on the SUV resulted in WAD measurements slightly less than the stature, which means that not only does the dummy not exhibit sliding (like in the sedan tests), but that the dummy did not evenly wrap around the vehicle in the SUV cases. (Figure 5).

High speed video images (1 kHz) from each test were analyzed to determine the time of head-to-vehicle contact. Because of the temporal resolution (1 ms) of the video images, the exact time of head contact to the vehicle could not be determined. However, the last imager frame prior to head contact (HC1) and the first imager frame after contact (HC2) initiated were determined, and since the change in the resultant head linear velocity relative to the vehicle velocity (Appendix Figure A1) over this short (1 ms) time interval was relatively high, head impact velocities are reported as the average ("Impact Velocity" in Table 2) and as the average and range over the time interval (Figure 7). Head impact velocities exceeded the vehicle velocity between 6% (P3) and 43% (DA1) in the sedan cases. In the SUV cases, the head impact velocities were less than the vehicle velocity in the repeated dummy tests (6%-16%) and in one PMHS test (4%), but higher than the vehicle velocity in the adjusted dummy tests (3%-8%) and in the other PMHS test (9%).

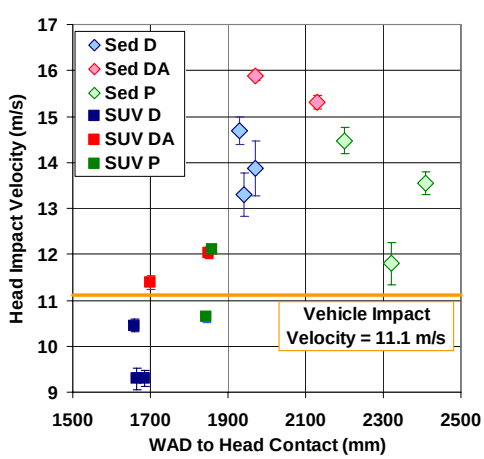

Figure 7. Impact velocity vs. WAD to head contact for all tests.

With regard to the risk of injury resulting from linear acceleration, the 15 ms Head Injury Criteria (HIC15) (Table 2)–calculated from the head CG resultant linear acceleration (Appendix Figure A1)–was compared to the impact velocity (Figure 8) and the WAD to head contact (Figure 9). In general, HIC15 values increased with head impact velocity for each vehicle with some exceptions.

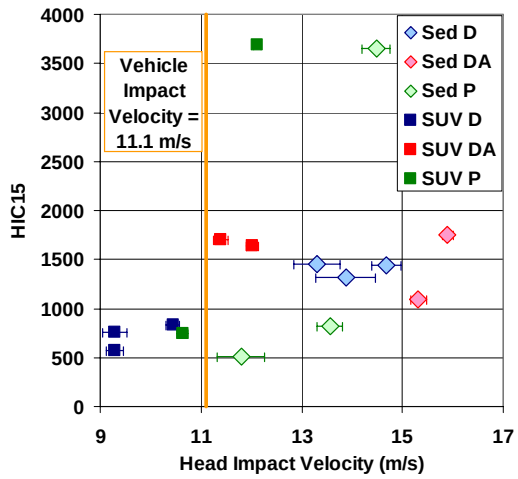

Figure 8. HIC15 vs. head impact velocity for all tests.

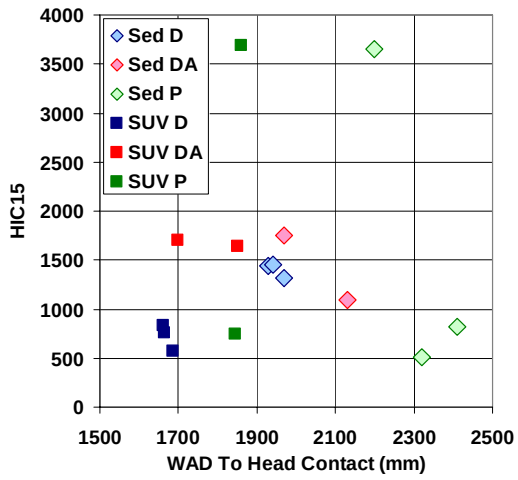

Figure 9. HIC15 vs. WAD to head contact for all tests.

The first adjusted dummy test (DA1) on the sedan resulted in the highest impact velocity (15.89 m/s), which was only slightly higher than that in the repeated dummy tests (13.3-14.7 m/s). This resulted in DA1 having only a slightly higher HIC than the repeated tests (1749 vs. 1321-1447) since head contact was in a similar location in each case (WAD 1930-1970 mm). In DA2, the dummy sustained a substantially lower HIC15 (1091) by impacting the windshield farther up (near the center) at a slightly lower impact velocity (15.9 vs. 15.3 m/s) than DA1. The second PMHS endured head impact at location similar to in DA2 and a lower velocity (14.48 vs. 15.89 m/s), yet it sustained a much higher HIC15 (3647 vs. 1091) than DA2. While the other two

PMHS, which had head impacts to the top third of the windshield (12 and 21 cm higher up than P2), sustained head impacts at lower velocities (11.8 and 13.6 m/s) and recorded drastically lower HIC15 values (824 and 511).

The lowest impact velocities of all of the cases in this study were sustained by the dummy in the repeated SUV tests. Although the dummy sustained HIC values that were only among the lowest recorded in the study. In SUV DA1 the dummy sustained a higher HIC15 than in the repeated dummy tests (1704 vs. 577-826) despite impacting the vehicle at a similar location and only a slightly higher impact velocity (11.4 vs. 9.3-10.5 m/s). Raising the dummy up by 7 cm between DA1 and DA2 resulted in a 15 cm increase in WAD to head impact, and a slightly higher impact velocity (11.4 vs. 12.0 m/s) yet a slightly lower HIC15 (1642 vs. 1704). Looking at the PMHS SUV tests, there is a large discrepancy in HIC values between the two tests (3694 and 745) despite having similar impact locations (rear 10% of the hood) and a small difference in impact velocity (12.11 m/s vs. 10.64 m/s). Furthermore, DA2 and P1 have similar impact locations and similar velocities, but DA2 has a substantially lower HIC15 (1642).

By examining the vehicle hood and underhood components in the area of the impacts, it became clear that both the SUV PMHS (and SUV DA2) endured head impacts at a location on the vehicle hood just above the passenger compartment-engine compartment firewall. It is hypothesized that this structure is very stiff, and thus has substantial influence on HIC15 values. Further analysis of the video images showed that the chin of P2 contacted the right arm/shoulder 4-5 ms prior to contacting the hood. It is hypothesized that the head/arm impact resulted in the substantially reduced HIC15 value, and that if the head/arm impact had not occurred, the HIC15 value recorded by SUV P2 would be similar to that recorded by P1.

Linear Kinetics

Dummy neck forces (Appendix Figure A2) at head impact (HC1) were dominated by z-direction forces, which exceeded 2300 N in every test in this study, 2500 N in all but two tests, and 3000 N in four tests (Figure 10). Neck forces are presented as forces applied to the head, so the positive z-forces at impact indicate significant neck tension. X and y-forces were all below 400 N at impact, and on average, x and y-forces were only 4% and 10% of the of the tensile (z) forces, respectively. The repeated dummy tests resulted in the highest tensile forces at impact, followed by the adjusted SUV tests, and lastly by both the adjusted sedan tests and the repeated SUV tests, which sustained similar tensile forces at impact. Overall however, the average tensile force at impact was 2902 N with only a 15% coefficient of variation across all tests despite differences in vehicle geometry. Similar coefficients of variation in tensile force, 17% and 10% for the sedan and SUV tests respectively, were seen when considering impacts only with the same vehicle.

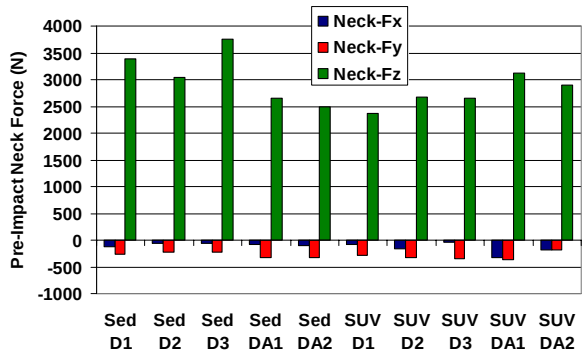

Figure 10. Dummy neck forces at the time of head contact (HC1).

Tensile forces similarly dominate neck forces throughout the interaction between the head and the vehicle. It is difficult to discern a robust kinematic marker for the end of the interaction time, so to examine the effect over the period of head-vehicle interaction, neck forces were averaged over the times used to calculate HIC15 (Figure 11). While z-direction forces still dominate neck forces throughout impact (1600-2500 N), x and y-forces were higher on average at 6% and 25% of the tensile force, respectively. The difference in tensile impact forces by test type is less clear than in the pre-impact forces. Overall, the average tension in the neck during the impact interaction was 2155 N with only 14% coefficient of variation across all tests. Similarly also, averaged tensile forces had only 16% and 12% coefficients of variation when considering sedan and SUV cases separately.

In contrast to neck forces, impact forces (Appendix Figure A2) are dominated by y-direction forces resulting from the vehicle impacting the right lateral side of the head. When impact forces are averaged over the times used to calculate HIC15 (Figure 12), the data show that in the SUV cases (except DA2) x-direction forces are commensurate with y-forces, but that y-forces are much larger than x-forces in the sedan cases. In the sedan cases, averaged y-impact forces were only slightly higher, on average, than z-neck forces (2590 vs. 2112 N). However, in the case of the SUV, averaged neck tensile forces were substantially

larger, on average, than y-impact forces (2199 N vs. 1381 N). This difference is still apparent, yet to a lesser degree, when comparing y and z-neck forces with x and y-impact forces in the SUV cases.

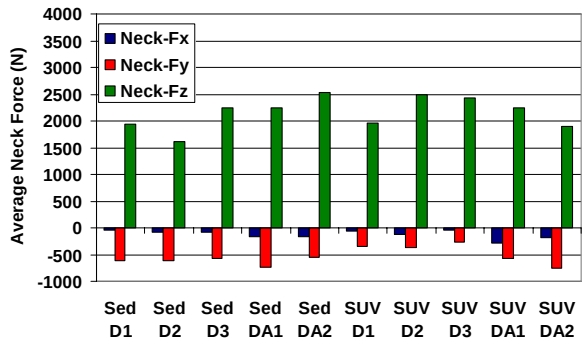

Figure 11. Dummy neck forces averaged over the times used to calculate HIC15.

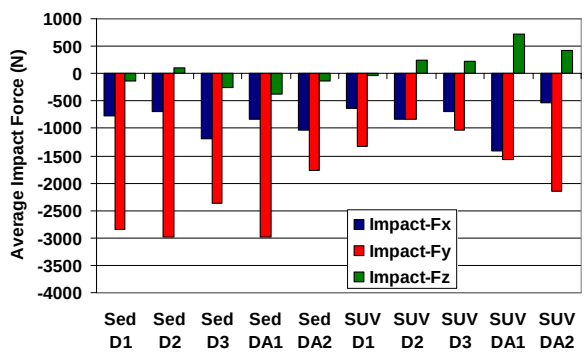

Figure 12. Dummy head impact forces averaged over the times used to calculate HIC15.

While there was no way to determine the neck or impact forces applied to the head during impact, Equation 1 and Equation 2 suggest that comparing local-frame accelerations between the dummy and PMHS tests, can shed light on the forces in the PMHS tests (Figure 13). In both Sed DA1 and SUV DA2, for example, the dummy shows that there are high z-accelerations at the time of impact (71 and 73 g, respectively), with virtually no x or y-direction accelerations (between 2 and 16 g). Similarly, there are high z-direction neck forces at the time of impact in both cases, but there was virtually no x and y-direction forces. Similarly in the PMHS, examining Sed P1 and SUV P1 for example, z-direction accelerations are relatively high at impact (54 and 80 g, respectively), and x and y-direction accelerations are lower (30 and 12 g in Sed 1, and 21 and 6 g in SUV 1, respectively), but slightly higher than in the dummy tests.

During the head-vehicle impact interaction, the dummy data shows that the z-direction acceleration and neck force reduces to zero by t_2 with the z-direction impact forces remaining small. Despite the smaller magnitude, the z-direction impact force in Sed DA1 opposes the z-direction neck force. However, in the case of the SUV, the opposite occurs and the z-neck force points in the same direction as the z-impact force. In contrast to the dummy tests, the z-direction PMHS accelerations remain relatively high throughout the interaction.

During the interaction, y-direction accelerations and impact forces in the dummy grow and remain relatively high, with smaller, yet still not negligible, y-direction neck forces, which point in the same direction as the impact force in both cases. The same is true for the x-direction accelerations and impact forces, but their magnitude is lower than those measured in the y-direction. Similarly in the PMHS tests, y-direction and x-direction accelerations grow and remain high throughout the interaction, with the y-accelerations being higher than the x-accelerations.

Overall, the averaged (between t_1 and t_2) resultant neck forces in the dummy were 61%-115% and 95%-190% of resultant impact forces in the sedan and SUV cases, respectively. On average, resultant neck forces were 79% and 128% of resultant impact forces in the sedan and SUV cases.

ANGULAR KINEMATICS

Resultant angular velocity and angular acceleration time histories (Appendix Figure A2) show that angular velocities are relatively high at the time of impact, and angular accelerations reach high values as a result of impact. Angular velocities at the time of impact are close to, or equal to, peak angular velocities measured in all tests. In general, the subjects reached peak angular accelerations during head-vehicle impact that spanned a large range between 4522 rad/s^2 (Sed P3) and 39126 rad/s^2 (SUV DA2). Averaging over the times used to calculate HIC15 (t_1-t_2), the dummy predicted higher angular accelerations in the sedan tests than in the SUV tests, despite having similar peak angular velocities in some cases (Figure 14). In the PMHS cases on the other hand, averaged angular accelerations were similar with one high case for each vehicle (~15600 rad/s^2) and the other cases lower (2300-4300 rad/s^2). Interestingly though, the peak angular velocities measured in the sedan PMHS tests were less than those measured in the SUV PMHS tests.

Furthermore, it is interesting to note that, other than in the adjusted dummy tests on the SUV, all of the tests showed that HIC15 and averaged angular acceleration

were well correlated (Figure 15). Additionally sedan test P2 and SUV test P1 resulted in very similar and quite high HIC15 and peak angular acceleration values, whereas the other PMHS tests predicted lower levels of injury risk.

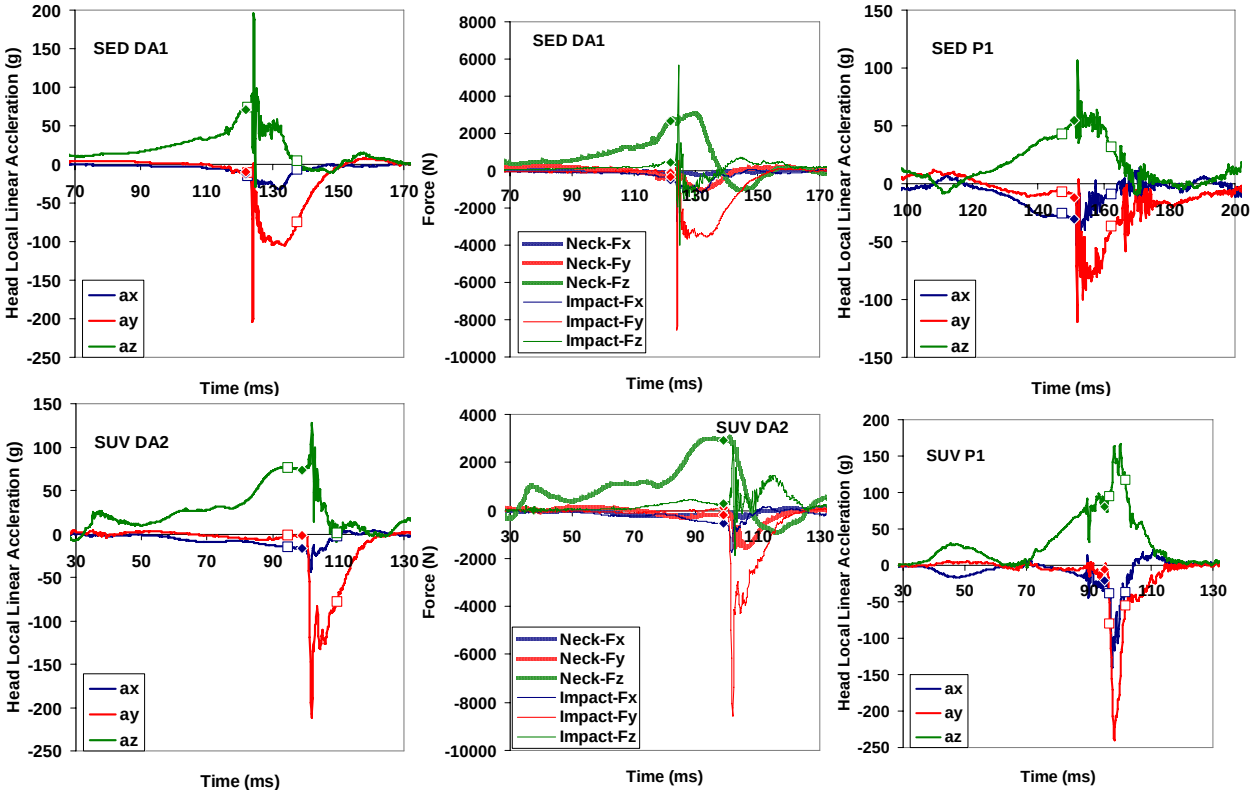

Figure 13. Head local accelerations from a sedan (top) and an SUV (bottom) dummy test (left), with neck and head impact forces (center), compared to head local accelerations from two PMHS tests (right). Times used to calculate HIC values are shown in each plot with squares, and the head impact time (HC1) is shown with a diamond.

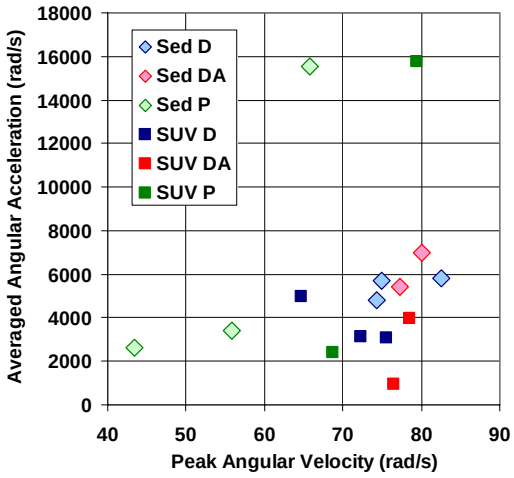

Figure 14. Resultant angular acceleration averaged over t_1-t_2 vs. peak angular velocity for all tests.

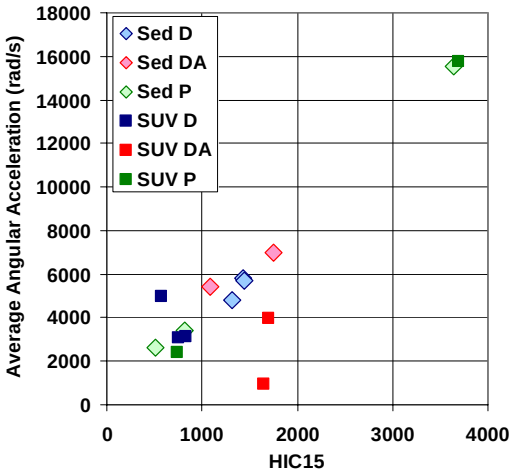

Figure 15. Resultant angular acceleration averaged over t_1-t_2 vs. HIC15 for all tests.

DISCUSSION

If head injury risk is measured in vehicle/pedestrian collisions using the linear acceleration (which determines HIC15) during interaction with the vehicle, solving Equation 2 for the head acceleration vector

$$\mathbf{a} = \frac{\mathbf{F_I}}{m_{head}} + \frac{\mathbf{F_N}}{m_{head}} \qquad (3)$$

shows that head injury risk is equally affected by the forces applied to the head through the neck, and by the forces applied to the head by the vehicle. Neck forces were shown to be dominated by z-direction (tensile) forces that increase to high levels well prior to head impact, and remain at relatively high levels throughout the impact interaction. High tensile neck forces prior to impact are easily explained by the overall kinematics of the subjects (Kerrigan et al. 2005a and Kerrigan et al. 2005b). The subjects' upper bodies undergo rotations about the x (anterior-posterior) axis with center of rotation near the pelvis. This results in the head, which is farthest from the pelvis, having the highest linear velocity, and its inertia causing high tensile forces in the neck. Okamoto and Kikuchi (2006) showed similarly high tensile forces in the dummy neck prior to and at the time of head impact (~1500 N and ~4000 N in SUV and sedan impacts, respectively).

Since the distribution of neck forces at impact (high z-force and low x and y-forces) does not change dramatically during interaction with the vehicle, it can be concluded that head impact with the vehicle does not dramatically affect the force transmission from the neck to the head. Impact forces, on the other hand, are dominated by y-direction (lateral) forces, with somewhat high forces also in the x-direction, and virtually no forces measured in the z-direction. Since these forces are caused by vehicle impact, it makes sense that they are directed in the right-to-left lateral direction and in the anterior-to-posterior direction because head impacts occur to the right-anterior side of the head (Figure 5).

Equation 3 also shows that when impact forces and neck forces point in the same direction, the effect on the acceleration is additive. Another way of saying this is that when the neck force points in the same direction as the impact force, the neck force results in increased head acceleration, and when the forces have opposite polarities, neck forces decrease head accelerations. Data from this study shows that the neck force has an additive effect on the acceleration magnitude, on average, in the x, and y directions in all of the tests and in the z-direction in the SUV tests. In the sedan tests, on average, the z-impact force opposes the neck force, but is only 8% of the neck force (162 N vs. 2112 N) the mitigating effect on the z-acceleration is low.

In this study, all of the force applied to the head through the neck is assumed to be measured by the dummy's upper neck load cell, when the structure of the dummy (Figure 16) as well as the presence of impact forces prior to head contact (Appendix Figure A2) suggests that this is not true. Firstly, the dummy has anterior and posterior cables designed for the THOR dummy to increase the flexion-extension stiffness of the neck, that provide for a load path between the head and the neck that is parallel to that which passes through the neck load cell. While the THOR dummy contains load cells to measure the tension in the cables, the Polar-II dummy did not. Since the cables can only support loads in tension, data from this study show that neck tensile loads are underestimated. The time histories of z-direction impact forces (Appendix Figure A2) show that a tensile "impact" force (between 67 and 420 N) was measured prior to impact in all of the tests.

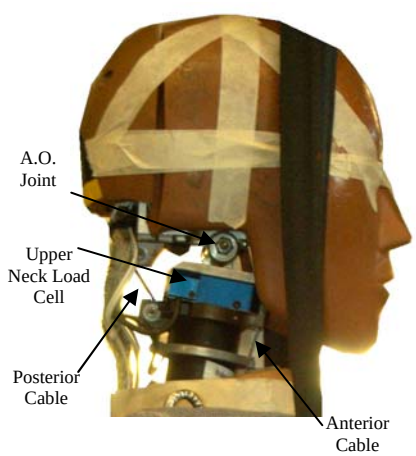

Figure 16. Photo depicting Polar-II head/neck connection and instrumentation.

Additionally, the dummy neck has a pin joint between the dummy neck and the head (A.O. joint), which permits the head's coordinate system to be rotated about the y-axis between -8 degrees (extension) and 25 degrees (flexion). Thus the orientation of the head's acceleration coordinate system was not necessarily aligned with the neck's coordinate system. This difference explains why there are impact forces measured in the x-direction prior to impact (between 80 and 560 N). Negative x-direction forces applied through the neck that result in these pre-contact "impact" forces, suggest that prior to impact the A.O. joint is in extension, and if the neck forces could be

corrected for A.O. joint angle (which is measured by a potentiometer in THOR) these x-direction impact forces would actually be recorded as increased tensile forces.

While it is not possible to measure neck forces in the PMHS directly, it is hypothesized that force transmission from the neck to the head is different in PMHS than in the dummy. A primary justification of this hypothesis can be explained by the lack of active musculature. Since the PMHS lacks active musculature, and the dummy's neck was designed to have the stiffness of a living human with active musculature (Akiyama et al. 2001) there are some differences in the head trajectory (Kerrigan et al. 2005a and Kerrigan et al. 2005b) and head linear and angular velocity (Appendix Figure A1) between the dummy and the PMHS. The linear velocity time histories show that PMHS reach lower peak head velocities than the dummy, and the angular velocity time histories show an early peak not seen in the dummy tests, which results from the motion of the thorax being out of phase with the motion of the head. In other words, as the thorax of the dummy rotates down toward the car, the relatively stiff neck of the dummy keeps the head in line with the thorax (see Kerrigan et al. 2005a and Kerrigan et al. 2005b for more high speed imagery from the tests). But in the PMHS tests, as the thorax rotates, the inertia of the head and relatively low stiffness of the neck caused a delayed reaction of the PMHS head.

Further evidence of the difference in force transmission between the head and neck of the PMHS and dummy can be seen in the differences in head impact dynamics between the DA2 dummy tests and PMHS tests Sed D2 and SUV D1. Despite sustaining similar head impact velocities at similar (or the same) impact location, DA2 in the sedan and SUV resulted in much lower HIC15 values than in the Sed P2 and SUV P1. Since impact accelerations are determined by neck and impact forces (Equation 3), the sum of the neck and impact forces must have remained much higher during the impact in Sed P2 and SUV P1 than in the DA2 tests. While it is not possible to know whether it was the neck force or the impact force (or both) that was higher in the PMHS tests, comparing accelerations and impact forces in two dummy tests (Figure 13) showed that z-direction accelerations correlated with z-direction neck forces before and during head impact, and that x and y-direction accelerations correlated with impact forces during the head impact. In comparing SUV P1 with SUV DA2, while y-direction accelerations appear to remain at similar levels through out the impact, x and z-direction accelerations in the PMHS remain higher than those in the dummy tests, which suggests that both neck forces and impact forces were higher in the PMHS. Ideally though, to provide a more accurate estimate of this difference, a universal (not representing any particular vehicle) with instrumented impact surfaces should be used to measure impact forces directly.

It is hypothesized that SUV P2 would have resulted in similar impact dynamics as those seen in SUV P1, had it not endured a head/arm impact prior to (and during) the head/hood impact. Not only did the arm impact reduce the linear acceleration and HIC15 value, but it reduced the peak and averaged angular acceleration values.

In comparing head impacts to the sedan and to the SUV, the difference in impact velocity between the two vehicles, on average, showed that the dummy impacted the sedan at a 39% higher velocity in the sedan tests than in the SUV tests (14.6 vs. 10.5 m/s). Looking at the forces, on average, averaged resultant neck forces were similar between the two vehicles, but impact forces were 57% higher in the sedan tests than in the SUV tests (2930 vs. 1862 N). The higher impact velocities resulted in higher impact forces causing the dummy to predict higher HIC15 values and higher angular accelerations in windshield impacts in the sedan tests than in hood impacts in the SUV tests. This result is further supported by epidemiology data showing that the windscreen causes greater Harm to pedestrians than any other vehicle structure (Fildes et al. 2004) and almost half of all AIS 2-6 head injuries are caused by the windscreen (Mizuno 2003).

CONCLUSIONS

In the current study, head impact dynamics experienced by pedestrians struck by a small sedan and a large SUV were examined using data from impacts with both a pedestrian dummy and PMHS. Despite analyzing only lateral impacts with two vehicle geometries at 40 km/h, the results and analyses presented in this study provide insights into pedestrian head impact dynamics that can be used to improve passive and active pedestrian injury countermeasures.

In general, the results of the dummy tests showed that the Polar-II dummy is repeatable but that differences in the pre-test position, support and clothing of the dummy can dramatically affect head impact dynamics, with a greater effect seen in the SUV tests compared to the sedan tests. Additionally, the dummy shows good biofidelity in comparing it to the PMHS tests, however, differences in stature and neck stiffness between the PMHS and dummy affect head dynamics before and during head impacts

The data also showed that, for both vehicles, dummy neck forces contribute a substantial and additive effect to head impact accelerations because the component-wise neck forces point have the same polarity as the component-wise impact forces, and because the neck forces are of comparable magnitude to the impact forces: neck forces were, on average, 79% and 128% of resultant impact forces in the sedan and SUV cases, respectively. In the case of the SUV, averaged resultant neck forces exceeded averaged impact forces, suggesting that neck forces affect head accelerations more than impact forces in the SUV.

While inclusion of the PMHS data complicates the relationship, the dummy predicted higher HIC15 values and higher angular accelerations in windshield impacts in the sedan tests than in hood impacts in the SUV tests. This difference is due to the higher impact velocities in the sedan tests compared to the SUV tests (14.6 m/s vs. 10.5 m/s), which result in higher impact forces transmitted to the head by the vehicle.

REFERENCES

Akiyama A, Okamoto M, Rangarajan N. (2001) Development and application of the new pedestrian dummy. Paper 463, 17th Conference on the Enhanced Safety of Vehicles, Amsterdam, The Netherlands.

Fildes B, Gabler HC, Otte D, Linder A, Sparke L. (2004) Pedestrian impact priorities using real-world crash data and harm. 2004 International Conference on the Biomechanics of Impacts (IRCOBI), Graz, Austria.

Kam C, Kerrigan J, Meissner M, Drinkwater C, Murphy D, Bolton J, Arregui C, Kendall R, Ivarsson J, Crandall J, Deng B, Wang JT, Kerkeling C, Hahn W. (2005) Design of a full-scale impact system for analysis of vehicle pedestrian collisions. Paper 2005-01-1875, Society of Automotive Engineers, Warrendale, PA.

Kerrigan J, Crandall J, Deng B. (2007) Pedestrian kinematic response to mid-sized vehicle impact. International Journal of Vehicle Safety. 2007; 2(3): 221–240.

Kerrigan, J, Crandall, J, Deng, B. (2008a) A Comparative Analysis of the Pedestrian Injury Risk Predicted by Mechanical Impactors and Post Mortem Human Surrogates. Stapp Car Crash Journal, 52, pp. 527-567.

Kerrigan J, Kam C, Drinkwater C, Murphy D, Bose D, Ivarsson J, Crandall J. (2005a) Kinematic Comparison of the Polar-II and PMHS in Pedestrian Impact Tests with a Sport-Utility Vehicle. 2005 International Conference on the Biomechanics of Impacts (IRCOBI), Prague, Czech Republic.

Kerrigan J, Murphy D, Drinkwater D, Kam C, Bose D, Crandall J. (2005b) Kinematic corridors for PMHS tested in full-scale pedestrian impact tests. NHTSA, Paper 05-0394, Proc. 19th Conference on the Enhanced Safety of Vehicles (ESV), Washington DC, United States.

Kerrigan J, Rudd R, Subit D, Untaroiu C, Crandall J. (2008b) Pedestrian lower extremity response and injury: a small sedan vs. a large sport utility vehicle. Paper Number 2008-01-1245, Society of Automotive Engineers, Warrendale, PA.

Mizuno Y. (2003). Summary of IHRA pedestrian safety WG activities (2003)-proposed test methods to evaluate pedestrian protection afforded by passenger cars. NHTSA Paper 580, Proc. 18th Conference on the Enhanced Safety of Vehicles (ESV), Nagoya, Japan.

Neal-Sturgess CE, Carter E, Hardy R, Cuerden R, Guerra L, Yang J. (2007) APROSYS European In-Depth Pedestrian Database. Proc. 20th Conference on the Enhanced Safety of Vehicles (ESV), Lyon, France.

Okamoto Y, Kikuchi Y. (2006) A study of pedestrian head injury evaluation method. Proc. 2006 International IRCOBI Conference on the Biomechanics of Impact, pp. 265-276.

Padgaonkar AJ, Krieger KW, King AI. (1975) Measurement of angular acceleration of a rigid body using linear accelerometers, J. Appl. Mechanics, 42, 552–556.

Robbins, D.H. (1983) Anthropometric Specifications for Mid-Sized Male Dummy, Volume 2. Report number UMTRI-83-53-2, University of Michigan Transportation Research Institute, Ann Arbor, MI.

Society of Automotive Engineers, Inc., “Instrumentation for Impact Tests,” SAE J211/1 MAR95, March 1995, 10 p.

APPENDIX

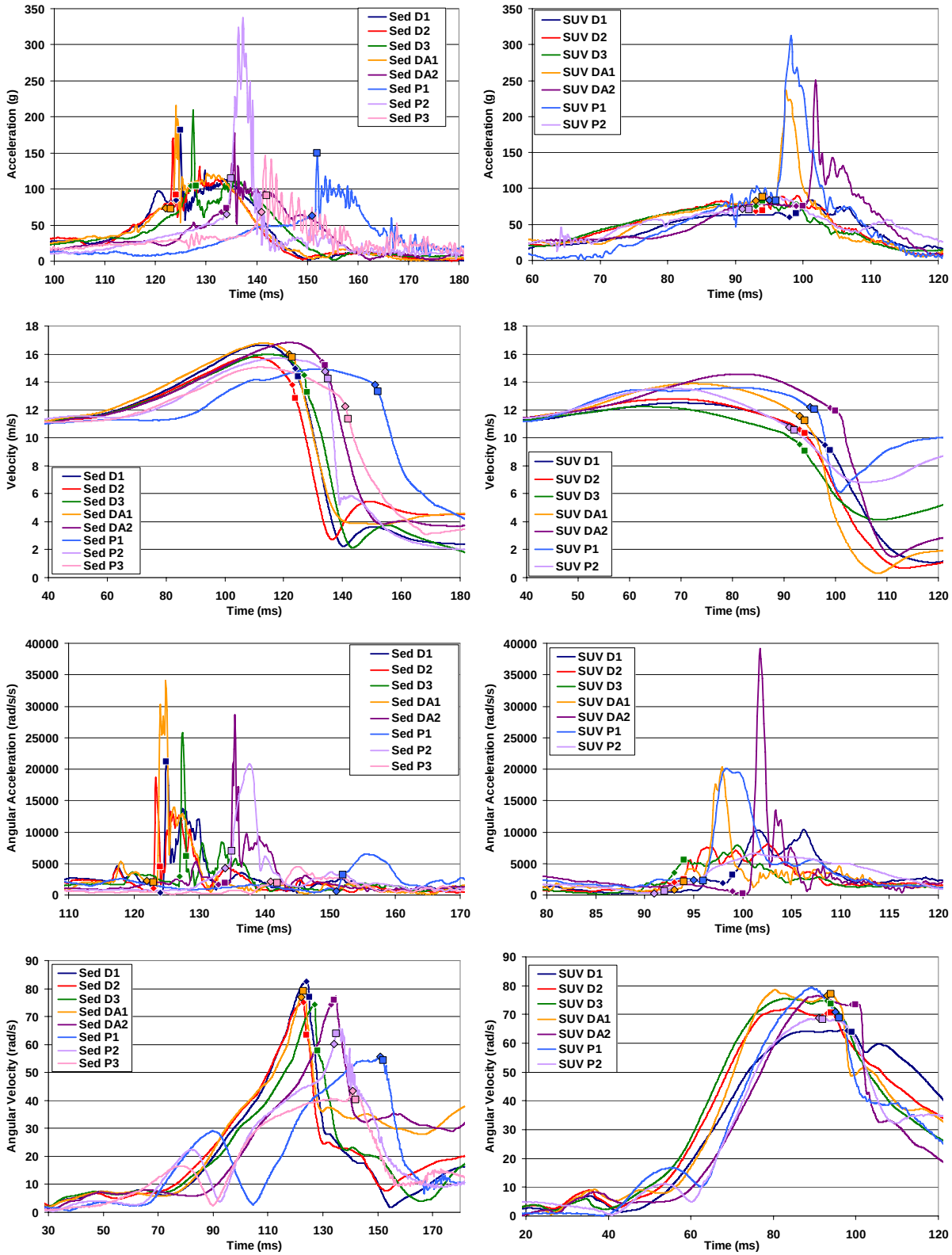

Figure A1. Head resultant linear acceleration and velocity, and angular acceleration and velocity time histories from the sedan (left) and SUV (right) tests. The diamond indicates HC1 and the square indicates HC2.

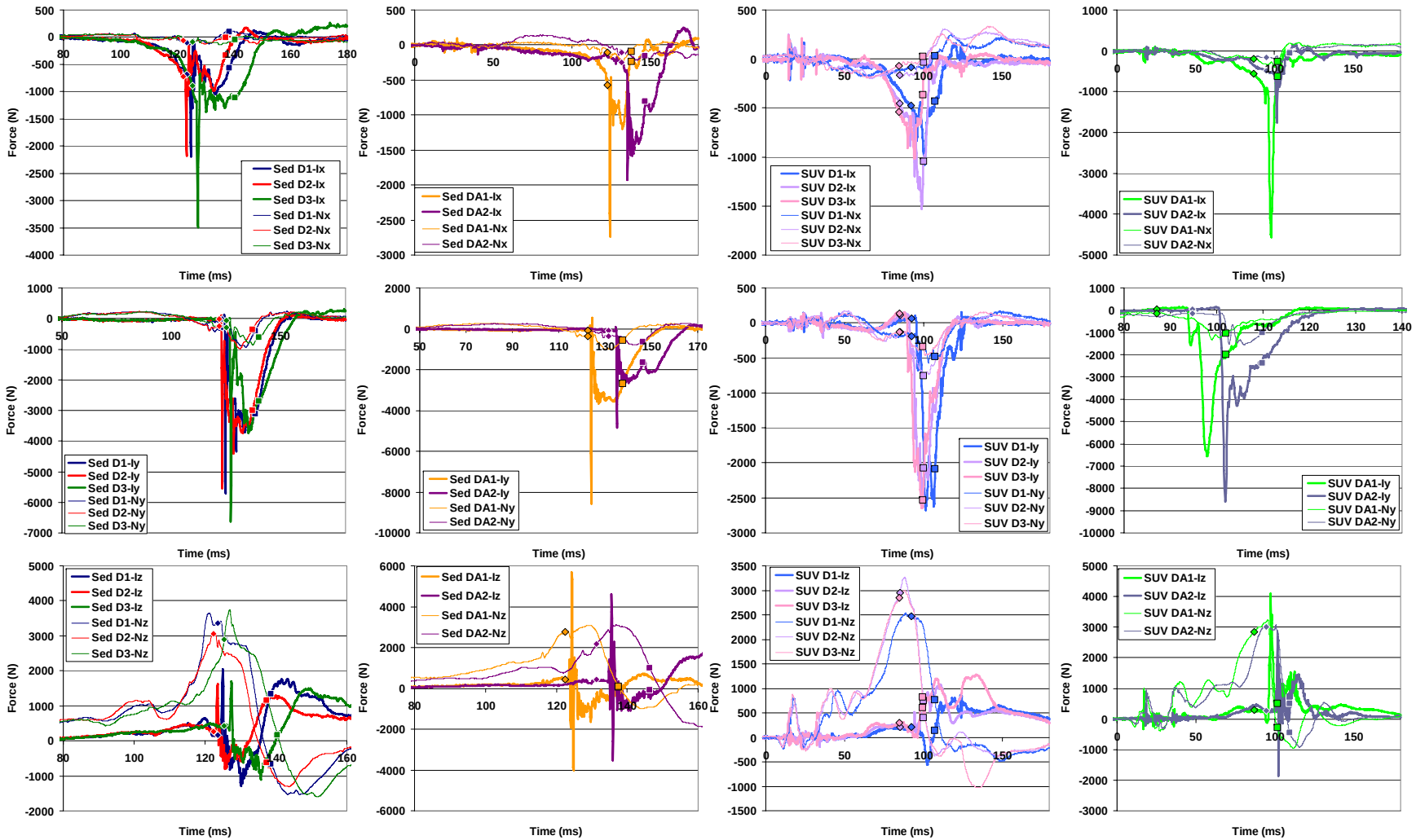

Figure A2. Impact forces ("Ix", "Iy", and "Iz") and neck forces ("Nx", "Ny", and "Nz") applied to the head. Forces are in the head's local coordinate system as defined by SAE J211 (Figure 4). The diamond and square indicate HIC calculation times t_1 and t_2, respectively. Note that time and force scales very.